ACS OMEGA

http://pubs.acs.org/journal/acsodf

Article

Decomposition of Chemical Warfare Agent Simulants Utilizing Pyrolyzed Cotton Balls as Wicks

Bryan A. Lagasse, Laura McCann, Timothy Kidwell, Matthew S. Blais,* and Carlos D. Garcia*

Cite This: *ACS Omega* 2020, 5, 20051−20061

Read Online

ACCESS | Metrics & More | Article Recommendations | Supporting Information

ABSTRACT: A simple method to improve the thermal decomposition of chemical warfare agent simulants is reported. Utilizing pyrolyzed cotton balls as a substrate for the delivery of an incendiary agent into a bulk volume of chemical warfare agent simulants, significant enhancements in the burning rates were achieved with respect to either other wicks or the incendiary agent by itself. To perform the decomposition experiments and follow the reaction in real time, while still addressing the important safety considerations related to experiments involving chemical warfare agent simulants and incendiary agents, a simple instrument was assembled in a laboratory hood, where all experiments were performed. Under ambient conditions, this method was able to enhance the decomposition of simulants for both sulfur mustard (HD) and sarin (GB) chemical warfare agents. Overall, the proposed approach represents one of the simplest and more cost-effective ways to improve the decomposition of these dangerous substances, presenting options for field expedient and low-cost processes that could be applied in the near future to the safe destruction of an actual CWA.

INTRODUCTION

Chemical warfare agents (CWAs) were employed in modern conflicts dating back to World War I when sulfur mustard (bis(2-chloroethyl)sulfide), also known as HD, was first used to incapacitate large numbers of soldiers.[1−3] Sulfur mustard's primary method of incapacitation is through the production of highly unstable compounds, such as sulfonium, which then alkylate sulfhydryl or amino groups in proteins and nucleic acids.[1,4] This alkylation proceeds to cause further damage by preventing cellular glycolysis and eventually leading to necrosis, typically within an hour of exposure to the agent.[1] Despite its relatively low fatality rate,[1,5,6] exposure to even small doses of HD can cause extensive damage to the skin, eyes, and respiratory systems (blisters, swelling, and necrosis).[1,4] In contrast to HD, nerve agents such as *o*-ethyl *N*,*N*-dimethyl phosphoramido cyanidate (tabun or GA), (*R*,*S*)-propan-2-yl methylphosphonofluoridate (sarin or GB), and ethyl ((2-[bis{propan-2-yl)amino]ethyl}sulfanyl)(methyl)-phosphinate (VX) are considered to be extremely lethal and have the capability of killing large numbers of people within minutes, at the extremely low doses of 14 (of body weight), 24, and 0.04 $mg{\cdot}kg^{-1}$, respectively.[7−9] These nerve agents primarily interact with the muscular and nervous systems of the body by binding to acetylcholinesterase, thus preventing the hydrolysis of acetylcholine in the synaptic junction[8] and causing respiratory failure within minutes through rigid paralysis.[10,11] In addition to requiring only minuscule concentrations to cause catastrophic effects, some nerve agents are considered environmentally persistent due to their low volatility and poor solubility in water.[8,12,13] In 1997, the Chemical Weapons Convention established the Organization for the Prohibition of Chemical Weapons, which prohibited the use and production of CWAs. Unfortunately, these efforts have not prevented nonstate actors such as terrorist organizations and rogue nation-states from developing and/or utilizing these incredibly lethal substances. Two of the most recent highly publicized attacks occurred using nerve agents: 2017 in an assassination in Kuala Lumpur and 2018 during a failed assassination attempt in the U.K. On a greater scale, both chlorine-based and sarin agents have been used against military and civilian populations with devastating effects during the Syrian civil war, which started in 2012.[14] Based on the high degree of damage these agents can cause at extremely low concentrations, it is necessary to develop faster, inexpensive, and more effective means to decompose CWAs in large volumes.

It is accepted that environmental conditions (i.e., temperature, humidity, and wind) have a significant effect on the persistence of CWAs in the environment (i.e., ∼30 h for HD[15] and ∼65 h for GB[8,16]). These factors have contributed to the development of a variety of treatment methods, including physical[17] and physicochemical.[18,19] Among those, the U.S. Army sought to develop multiple methods for disposing of its chemical weapon stockpile with a focus on incineration or chemical neutralization.[20] Neutralization methods were initially abandoned, however, due to incomplete reactions and the large volumes of chemical waste produced, leading to incineration being selected as the preferred method for large-

Received: April 8, 2020
Accepted: July 13, 2020
Published: July 24, 2020

https://dx.doi.org/10.1021/acsomega.0c01619
ACS Omega 2020, 5, 20051−20061

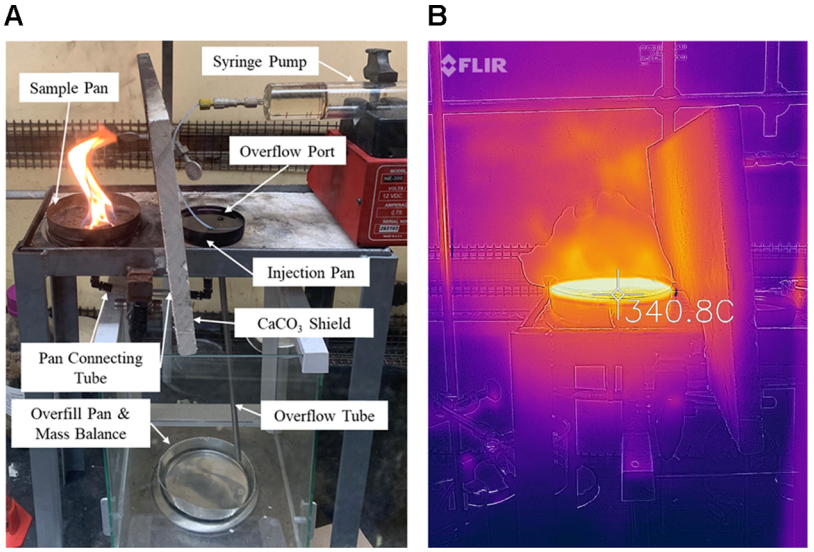

Figure 1. (A) Experimental setup for the burning of chemical warfare agent simulants while measuring the overflow. A fresh agent is pumped into the injection pan on the right side, while the napalm-coated pyrolyzed cotton balls were introduced to the sample pan on the left side. (B) Thermal image of the sample pan during one of the experiments. The image shows the spot used to estimate the temperature of the agent.

scale disposal.[21] Incineration and thermal decomposition methods remained the primary route for the U.S. Army to destroy large volumes of agents throughout the 1980s and 1990s[20,21] until they were discontinued due to their large costs.[20,21] While incineration at high temperatures is effective at treating large stockpiles, the process is also slow and requires extensive equipment and materials to achieve both incineration and testing of the remaining materials. The U.S. Army estimated that it would take more than 5 years at some of the chemical storage facilities to complete the decontamination process through large-scale incineration.[20] These restraints also limit the effectiveness of current incineration methods toward field expedient or on-site destruction of chemical weapons that may be discovered during either armed conflict or by regulatory agencies during inspections. Owing to these factors, recent research has found that metal organic frameworks (MOFs) can effectively degrade a variety of chemical warfare agents.[19,22,23] Highly oxidized porous carbon surfaces have shown to decompose simulants for HD up to 80% decomposition after 24 h of contact with the oxidized carbon surfaces.[24] While these methods address the need for providing improved protection for individuals who encounter CWAs, they have limited application for large-scale degradation of agents, which are typically addressed through chemical treatment.[25] Of these methods, hydrolysis and oxidation are among the most common methods currently used to decompose chemical agents.[3,18,25−28] While these approaches are generally effective, their efficiency is heavily dependent on the reaction conditions (i.e., pH and temperature), and they also require a large excess of reagents to achieve acceptable levels of decontamination.[16,26] In addition, these processes also generate large volumes of waste and a number of toxic byproducts.[15,16,26,29] Aiming to improve the rate and/or yield of these reactions, recent studies of the hydrolysis of CWAs have focused on the use of catalysts, such as silver nanoparticles or alumina substrates.[29,30] Despite these advances, there is a current need for simple methods for thermal degradation of bulk volumes of agents, with limited sample preparation or treatment.[31,32] Possible reasons for this dearth of research include the low flammability of some of these compounds, as well as the risk of producing hazardous byproducts.[33] In addition, the specific instrumentation and low-scale volumes (less than 20 μL in previous studies[31,32]) have not provided enough information to support field deployment of these strategies.

Aiming to address these limitations, we present a simple approach to bolster the decomposition of a variety of CWAs via open-flame combustion. The approach is based on the use of pyrolyzed cotton balls (PyCBs) acting as wicks, which, upon being soaked with napalm B (as the starting incendiary agent), are able to drive the decomposition to be self-sustaining (using the agent itself to fuel the combustion) under ambient conditions. The method represents a low-cost alternative to achieve combustion and thermal degradation of liquid chemical warfare agents, which can be scaled to accommodate bulk volumes of the agent. While the proposed method does not remove the requirement to process and clean the resulting smoke and atmosphere of potentially harmful byproducts, it does present a simple, inexpensive, and potentially deployable means of decomposition without the need for large-scale instruments. In this context, the presented three-dimensional carbon substrates could help the development of alternative highly porous, pyrolyzed organic materials to be deployed or developed on-site to sustain combustion of agents. In addition, enemy stockpiles of CWA are stored in reinforced structures, and airdrop munitions are a potential method of destruction. Because wood dunnage is typically present in such structures and will pyrolyze, wicking will occur from CWA pools. As such, this manuscript aims to determine the viability of the approach in a postexplosion destruction scenario.

PROTOCOL FOR DECOMPOSITION EXPERIMENTS

To perform the decomposition experiments and follow the reaction in real time, the experimental setup shown in Figure 1 was used. The system comprised a screw-driven syringe pump (NE-3000 Just Infusion syringe pump, New Era Pump Systems Inc., Farmingdale, NY) used to deliver the simulants, a 50 mL glass syringe (Fortuna Optima 7.140 Luer-Lock tip, Poulten & Graf GmbH, Wertheim, Germany), two stainless steel pans connected by plastic tubing, a calcium carbonate fire barrier, an

https://dx.doi.org/10.1021/acsomega.0c01619
ACS Omega 2020, 5, 20051−20061

overflow tube, a collection pan, and a digital balance (Mettler Toledo ME104E, Zaventem, Belgium) connected to a computer via a standard serial cable using the accompanying balance software (LabX Direct Balance, version 2.5). Alternative view angles of the experimental setup are included in the Supporting Information. Thermal images and videos were captured using an infrared camera (FLiR One Pro iOS version, FLIR Systems Inc., Wilsonville, OR) by pointing the measuring spot to the center of the sample plate (at the base of the flame) to estimate the temperature of the agent (Figure 1B).

Before each experiment, all pans and tubes were cleaned with methanol and allowed to dry completely to prevent contamination. The syringe was then loaded with 30−40 mL of the selected agent simulant to be studied. The syringe was secured to the pump, which was programmed for a delivery rate of 4.00 mL·min^{-1}. Next, ∼10 mL of the selected simulant was dispensed into the injection pan (the right pan in Figure 1) and allowed to equilibrate with the sample pan (the left pan in Figure 1) via the connection tubing underneath the pans. Any excess agent was drained (via the overflow tube) into the overfill pan (placed on the balance). This prefilling step reduced the overall time of the experiment by eliminating the necessity of reloading the syringe after the simulant equilibrated and filled up both pans to the level of the overflow tube. It is also important to note that the total volume of the sample used depended on the diameter of the pans. To limit the variance in the data, a constant pumping rate was used in all experiments and each iteration had an overflow period as an internal standard to compare the rate of overflow before and after burning was achieved. For the experiments described herein, the only variables were the diameter of the sample pan and the type of simulant used.

In all experiments, the change in the mass from the overflow of the simulant (i.e., from the injection pan and burning pans overflowing into the collection pan) was recorded as a function of time. This approach allowed for the determination of both the initial delivery rate prior to the initiation of combustion, whereby all of the sample overflowed into the collection pan, and the burning rate where the difference between the accumulated mass in the collection pan and the amount delivered into the system. A representative example of the data acquired is shown in Figures 2 and 3 (vide infra), where the mass in the overflow pan was recorded as a function of time.

As it can be observed in Figure 2, a linear increase in the overflow mass was observed at the beginning of the experiment, when the agent is pumped at a constant rate, before the ignition. This initial rate (solid black line, Figure 2) corresponds to the pumping rate of 4.00 mL·min^{-1}. Across all of the pans examined in this study, the average rate of overflow was 3.6 ± 0.5 mL·min^{-1}, with the smaller pans at 4.00 mL·min^{-1} rate and the larger pans at 3.25 mL·min^{-1} rate. This difference in flow rates was attributed to the increased volumes in the larger burning pans necessitating the pumping of more solution into the system to sustain combustion.

Once the ignited napalm-coated PyCB was introduced to the sample pan (after approximately 2 min, as shown in Figure 2), the simulant started to burn, and a clear decrease in the overflow mass was observed, as the simulant pumped into the system was burned and did not overflow. As a reference, the temperature at this stage was 250 °C (as estimated by the IR camera). By comparing the overflow rate with the pumping rate—extrapolated for the duration of the experiment (dashed line, Figure 2)—the amount and rate of the burning for the agent being studied can be determined. The overflow rate after ignition in each experiment was compared to the overflow rate before the ignited pyrolyzed cotton ball was introduced to the sample pan, to minimize the effects of variables such as small variations in the initial temperature of the pans and/or connecting lines (considered to be at room temperature). This internal comparison allowed for more accurate determination of the rate of burning for each experiment versus using the average rate of overflow for each pan size. These results were then used to calculate the difference between the input (overflow before ignition) and the output (overflow after ignition) amounts, which represents the mass of the simulant burned during the entire burning period, as shown in Figure 3. During the period of maximum burning, a significant increase in the temperature was also observed, reaching almost 400 °C (as estimated by the IR camera).

It is important to note that when the napalm-coated pyrolyzed cotton ball was ignited and introduced into the simulant, the change in the overflow rate was attributed to the

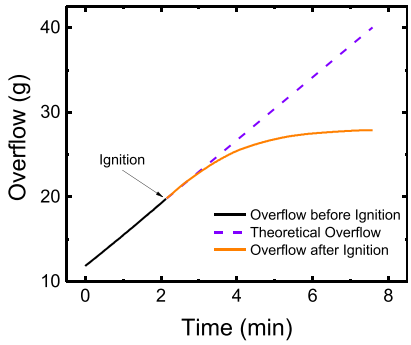

Figure 2. Representative example of the experiment designed to measure the overflow of the simulant before and after the introduction of the napalm-coated PyCB to a 9 cm diameter burning pan containing 2-chloroethyl ethyl sulfide (CEES). The figure shows the initial overflow rate before (black) and after (orange) the ignition of the napalm-coated pyrolyzed cotton ball. The figure also shows the extrapolation of the initial overflow (dashed line), from the input of the simulant by the syringe pump, throughout the duration of the experiment.

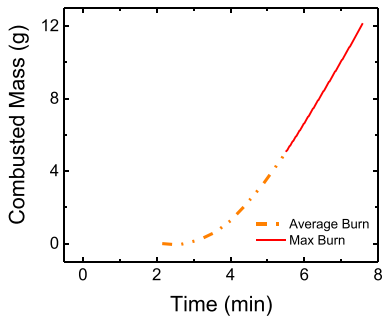

Figure 3. Representative example of the difference between the input and output (combusted amount) of the CEES simulant as a function of time, utilizing pyrolyzed cotton balls as a substrate in a 9 cm diameter sample pan. This shows when the ignited napalm-coated pyrolyzed cotton ball is first introduced to the sample pan, there is very little burning. After approximately 90 s, however, the rate of burning increases rapidly and approaches the maximum burn rate. During this period, the entire surface area of the sample pan is ignited, showing that the agent itself is serving as a fuel source for the combustion reaction.

https://dx.doi.org/10.1021/acsomega.0c01619
ACS Omega 2020, 5, 20051−20061

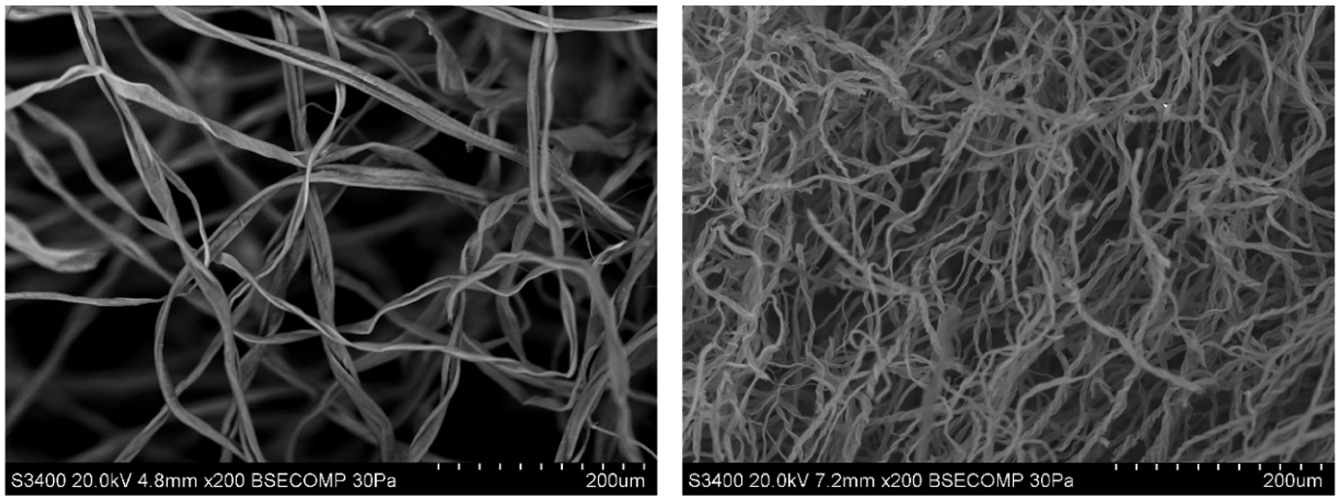

Figure 4. Scanning electron microscope images of nonpyrolyzed (left) and pyrolyzed (right) cotton balls showing the increased number of fibers per unit area and the decreased size of the individual fibers as a result of the pyrolysis process.

combustion of napalm. In control experiments where pyrolyzed cotton balls and napalm were burned without the presence of any chemical warfare agent or simulant, the pyrolyzed cotton balls and napalm burned for approximately 4 min. The self-extinguishing of the flame at this stage was attributed to the consumption of the napalm incendiary agent. It was observed that during these experiments the flame was restricted to only the pyrolyzed cotton ball and did not spread across the surface area of the pan. As the energy and heat from this reaction were transferred, the simulant was able to reach its respective ignition temperature and sustained thermal decomposition was achieved. The period of time before the sustained burning occurred was referred to as the initial burn period, as the burning was not completely fueled by the simulant (orange dotted line, Figure 3). The period of time, where a constant burning rate was achieved, was indicated by the linear region of the burned mass curve (solid red line, Figure 3) and was referred to as the maximum burning rate. The resulting data were evaluated for each experiment to determine the rate of maximum burning for the different simulants and as a function of the sample pan diameter. In all cases, data collection continued until either no simulant remained in the syringe pump or the flame in the burn pan self-extinguished.

Safety Considerations. Although the described experiments are performed with simulants (not live chemical warfare agents), these compounds are still toxic and may cause blisters or severe injuries. Extreme caution must be exercised when handling these compounds. To avoid possible injuries, all experiments were performed in a vented hood (average linear face velocity of 80−120 linear feet·min^{-1}), where all agents and waste products were properly contained. One shortfall of this experimental setup is that it allows for determining the rate of burning for a variety of CWA simulants, but not for determining the percentage of CWA decomposed. Just like with any experiment of this type, even when performed with simulants, that may serve to demonstrate the feasibility of a new concept, further studies and experimental designs are needed to determine and optimize the overall decomposition percentage before the methods could be applied to scale or be considered toward safe destruction of chemical warfare agents in practical scenarios. As this study focused on determining a method for achieving thermal decomposition without the presence of an incinerator or a continuous supply of an incendiary agent, these optimization experiments were outside the scope of this research and will be reported separately.

RESULTS AND DISCUSSION

Characterization of the Pyrolyzed Cotton Balls. To confirm the structural change of the cotton balls as a result of the pyrolysis process, both untreated cotton balls and pyrolyzed cotton balls were investigated via scanning electron microscopy (Figure 4). The nonpyrolyzed cotton ball is composed of large fibers (16 ± 4 μm in diameter) entangled to support the three-dimensional structure. Upon pyrolysis, the overall structure of the cotton ball was preserved, but a significant reduction in size (54%, from a diameter of 3.2 ± 0.2 to 1.7 ± 0.2 cm) and mass (92%, from 0.65 ± 0.03 to 0.052 ± 0.003 g) was observed. These values allowed estimating an average void volume of approximately 99% (considering a density of 2.1 g·cm^{-3} for pyrolytic carbon).

This decrease in the overall mass of the pyrolyzed cotton balls was attributed to the cleavage of low-molecular-weight oxygenated groups from the cellulose structures and the coalescence of the overall structure.[34] The resulting PyCB is therefore composed of a more rigid yet brittle three-dimensional network of carbon fibers. It is important to note that this small difference is not indicative of the dimensional changes occurring in each fiber, as the fibers in the PyCB appear to be twisted in comparison with the generally flat shape of the fibers observed in the nonpyrolyzed cotton ball (Figure S2). This difference limits the ability to accurately measure the true decrease in the size of the individual fibers due to pyrolysis (Figure S2). To better understand the change in the structure of the cellulose fibers and to confirm that the changes were homogeneous throughout the entire pyrolyzed cotton balls, a noncontact surface roughness assessment was conducted of a pyrolyzed cotton ball segmented into six pieces. These results revealed that the cellulose fibers are consistently an average size of 9.70 ± 1.23 μm. Furthermore, the surface roughness measurements were consistent for both the interior surfaces and the exterior surfaces of the cotton ball. This suggests that the pyrolyzation process results in uniform changes to the individual cellulose fibers. By examining the

https://dx.doi.org/10.1021/acsomega.0c01619
ACS Omega 2020, 5, 20051−20061

Table 1. Maximum Rates of Burning for CEES in a 5.5 cm Sample Pan with Various Incendiary Sources

	PyCB + napalm	wire mesh + napalm	PyCB + napalm pellet	unpyrolyzed cotton ball	unpyrolyzed cotton ball + napalm
maximum burning rate ($g \cdot min^{-1}$)	2.04 ± 0.16	2.19 ± 1.25	2.35 ± 0.52	1.21 ± 0.37	no measured burning

height profiles of the various segments, it was determined that there is significant layering within the pyrolyzed cotton ball, which creates voids and spaces within the spherical structure (Figure S3).

The surface area of the pyrolyzed cotton balls was conducted using the Brunauer–Emmett–Teller (BET) method, which revealed a surface area of 569.6 $m^2 \cdot g^{-1}$ (Figure S4). This surface area suggests that pyrolyzed cotton balls are between mesoporous carbon and activated carbon structures.[35,36] Furthermore, the Barrett–Joyner–Halenda (BJH) method revealed that the pore distribution of the pyrolyzed cotton balls centered around 19 Å (radius, Figure S5). This small pore size contributes to the pyrolyzed fibers serving as a wick, acting as an absorbent for the incendiary agent.

Finally, the pyrolysis process makes the cotton balls significantly more hydrophobic than nonpyrolyzed cotton balls, a change that was attributed to the removal of the polar functional groups from cellulose leaving almost pure carbon fibers,[34,37] which are significantly more hydrophobic and limit the capillary action of fibers transporting the liquid agent (Figures S5 and S6). This increase in hydrophobicity and limited capillary action are important for two reasons. First, the increased hydrophobicity allows the napalm mixture to coat the pyrolyzed cotton ball fibers without deforming the structure of the cotton ball. These observations are critically important for the selected application because the nonpyrolyzed cotton balls rapidly deformed when placed in the napalm mixture. PyCB samples were able to maintain their spherical shape and hold 1.2 ± 0.2 g of napalm without significant changes in shape. Second, as the pyrolyzed cotton balls experience less capillary transport than the unpyrolyzed variants, less of the liquid sample is adsorbed into the fibers. As there is less liquid absorbed into the fibers, it is posited that this allows more of the napalm mixture to combust and thereby increase the temperature of the liquid agent to reach the flashpoint and cause thermal decomposition. It is worth mentioning that nonpyrolyzed cotton balls were saturated in 2.5 ± 0.5 s when placed in a pan containing a simulant (both CEES and triethyl phosphate (TEP) had similar results), while the PyCB required 16 ± 5 s for the same level of saturation. These observations were critically important for the selected application as the unpyrolyzed cotton balls rapidly deformed when placed in the napalm mixture.

It is posited that the voids created in the pyrolyzed cotton ball coupled with the increased hydrophobicity are critical to the increased rate of maximum burning achieved with pyrolyzed cotton balls. This supports not only the napalm mixture coating the pyrolyzed cotton ball but also the decomposition of the chemical agent simulant as it is wicked along the pyrolyzed cellulose fibers. These voids allow the combustion of the napalm mixture that transfers energy to the liquid agent through conduction. The increased hydrophobicity allows the napalm mixture to more effectively coat the pyrolyzed cellulose fibers, which allows for more efficient energy transfer to the liquid agent. Additionally, since the pyrolyzed fibers are not absorbing the agent, the ignited napalm is not extinguished by the liquid simulant. As the fibers are coated with napalm, the agent is not absorbed into the cellulose fibers and rapidly approaches its flashpoint and undergoes a thermal decomposition reaction. While the exact mechanism varies based on the simulant, both CEES and TEP are primarily decomposed by a pericyclic reaction, which results in the expulsion of ethylene.[38−40] It is posited that the combustion of the ethylene formed allows the reaction to progress by continually adding energy to the system, until the simulant is fully consumed.

Control Experiments. To decouple the contribution of the napalm itself from the combustion process, experiments were conducted by dripping ignited napalm directly into a sample pan containing the selected agents. While the ignited napalm without any supporting substrate was able to initiate sustained burning of CEES, the burning rate was consistently lower than the corresponding value obtained with the napalm-coated PyCB. As a representative example, the maximum burning rate of CEES achieved in an 8.5 cm burn pan using napalm without a substrate was 2.7 ± 0.2 $g \cdot min^{-1}$, a 14% decrease compared to the burning rate with a PyCB substrate. Additionally, the amount of time during which sustained burning of CEES occurred was reduced from 90 ± 30 s (with the PyCB) to 40 ± 20 s (with no substrate). Furthermore, it took an average of 60 ± 10 s longer for CEES to reach a sustained burning rate when no pyrolyzed cotton ball substrate was present. It is also important to highlight that CEES is considered a flammable substance, while TEP, along with most nerve agent simulants, is considered to be nonflammable and does not ignite under most conditions. When napalm was used without a substrate, there was no observable ignition of the sample as the napalm was extinguished upon contact with the liquid agent. As TEP was only ignited and reached a sustained burn rate in the presence of a PyCB substrate, these experiments illustrate the importance of the wicking material in achieving the thermal decomposition of these organophosphate-containing compounds.

When the napalm was applied to a wire mesh as the substrate, it was possible to achieve some decomposition for both CEES and TEP. The maximum rate of burning achieved with the wire mesh and napalm above the simulant CEES was 2.19 ± 1.25 $g \cdot min^{-1}$, which was within the standard deviation of the maximum rate of burning achieved with napalm-coated pyrolyzed cotton balls at 2.04 ± 0.16 $g \cdot min^{-1}$ (Table 1). The wire-mesh-supported napalm suspended over TEP achieved a maximum burning rate of 0.85 ± 1.20 $g \cdot min^{-1}$, 53% of the maximum rate of burning of 1.60 ± 0.45 $g \cdot min^{-1}$ achieved when a pyrolyzed cotton ball wick was used. This suggests that while napalm alone is able to induce thermal decomposition of both simulants, it is necessary to have a substrate that prevents the napalm from being extinguished by the simulant. Conversely, while CEES was able to achieve burning from the ignited napalm being dripped into the simulant, this was attributed to the more volatile and flammable nature of CEES, versus the more stable organophosphate-based TEP simulant. This was in agreement with previous studies, as organophosphate-based compounds are commonly used as flame

https://dx.doi.org/10.1021/acsomega.0c01619
ACS Omega 2020, 5, 20051−20061

Table 2. Maximum Rates of Burning for TEP in a 5.5 cm Sample Pan with Various Incendiary Sources

	PyCB + napalm	wire mesh + napalm	PyCB + napalm pellet	unpyrolyzed cotton ball	unpyrolyzed cotton ball + napalm
maximum burning rate ($g \cdot min^{-1}$)	1.60 ± 0.45	0.85 ± 1.20	no measured burning	no measured burning	no measured burning

retardants due to the high stability of the organophosphate center.[41,42]

To demonstrate the advantages of PyCB toward the degradation of CWA simulants, thermal decomposition experiments were conducted in the presence of PyCB and compared to those performed with unpyrolyzed cotton balls. As unpyrolyzed cotton balls have a larger exterior surface area than the pyrolyzed cotton balls, the unpyrolyzed cotton balls were trimmed to ensure that a consistent mass of 1.2 ± 0.1 g of the napalm mixture was introduced into the sample. This control of the surface area was taken due to the large decrease observed in the pyrolyzed cotton balls, making it infeasible to obtain an unpyrolyzed cotton ball of the same mass as a pyrolyzed cotton ball while maintaining the same volume of napalm introduced to the system. The cotton balls were then coated in napalm, ignited, and placed in the sample pan. When the ignited cotton balls were placed in the pool of CEES in a 5.5 cm diameter sample pan, a maximum burning rate of 1.21 ± 0.37 $g \cdot min^{-1}$ was achieved. By comparison, the maximum burning rate for CEES in a 5.5 cm diameter pan with napalm-coated PyCBs was 2.04 ± 0.16 $g \cdot min^{-1}$. This represents a 40% increase in the maximum rate of burning compared to that of unpyrolyzed cotton balls. Interestingly, when an unpyrolyzed cotton ball was coated in napalm, ignited, and introduced to the CEES in the sample pan, it was not possible to determine a rate of burning from the experimental data. It is important to note that while burning was observed due to the napalm-coated unpyrolyzed cotton ball, there was no measured change in the overflow rate for the 2.5 min duration of the experiment, preventing a calculation of the mass of simulant burned. This phenomenon was attributed to the absorption of the agent by the unpyrolyzed cellulose fibers versus the decomposition. It is important to note that in all experiments where unpyrolyzed cotton balls were used, the unpyrolyzed cotton ball was heavily saturated with a simulant, even when the experiment was allowed to burn to completion. This suggests that while the unpyrolyzed cotton ball may be able to induce thermal decomposition of some of the agent, there would be agent remaining by physical containment in the cellulose fibers, which would require additional treatment. When pyrolyzed cotton balls were utilized, there was no measurable absorption of the agent into the pyrolyzed cotton ball fibers when burning was allowed to continue until all of the sample in the pan was allowed to burn to completion.

In all trials with TEP as the simulant using unpyrolyzed cotton balls, the flame was self-extinguished within 10 s, thus preventing the calculation of the burning rate (i.e., no significant change in the rate of overflow compared to the pre-ignition rate). This suggests that the pyrolyzation process is critical for the decomposition of nerve agent simulants due to the changes in the hydrophobicity and the lack of adsorption of the liquid simulant.

When pyrolyzed cotton balls were ground into a powder and formed into a pellet with napalm as the binding agent, it was possible to achieve thermal decomposition of CEES but not TEP. With CEES as the simulant in the 5.5 cm sample pan and the PyCB napalm pellet was introduced, the maximum burning rate achieved was 2.35 ± 0.52 $g \cdot min^{-1}$. While this control shows that burning was achievable with the pellets, there was a relatively high degree of deviation in the maximum burning rate between the two trials conducted. This suggested that while the pellets could achieve burning of CEES, the deformation of the pyrolyzed cotton balls introduces a level a variability into the preparation of the pellets that requires further optimization to ensure consistent results. Despite this variability, the rate of burning achieved with the pyrolyzed cotton ball and napalm pellets corresponds to a slight 15% increase over the maximum rate achieved with an undeformed napalm-coated PyCBs and suggests that the pyrolyzed cellulose fibers are important in achieving greater maximum burning. Conversely, the PyCB napalm pellets were not able to induce any burning in TEP, as the flame was extinguished within 10 s. It is posited that the difference in chemical structure, stability, and flammability of the simulants is the main factor in this difference in achieved burning.

While the precise mechanism preventing sustained ignition with the unpyrolyzed cotton balls is currently unknown, the described results present evidence that the structural changes in cellulose during the pyrolysis (carbonization, increase in contact angle, removal of oxygenated groups,[34] etc.) provide much more efficient support to promote the decomposition of both CEES and TEP. These results are summarized in Tables 1 and 2.

It is important to note that to conserve the chemical warfare agent simulants used in this study for the decomposition experiments with the pyrolyzed cotton balls all control experiments were conducted in duplicate. While this resulted in higher deviation in some experiments, these controls provided a baseline for understanding the impact of both the napalm and the pyrolyzed cotton balls in achieving sustained burning for different classes of chemical warfare agent simulants.

Decomposition of 2-Chloroethyl Ethyl Sulfide (CEES). While there is limited experimental research and data regarding the thermal degradation of both sulfur mustard and CEES, there is recent kinetic modeling of the reactions that predict the mechanism of decomposition.[43] This model predicts under combustion or pyrolysis conditions that the sulfur mustard (HD) molecule will decompose via a pericyclic pathway, cleaving the C−S bond to produce S−H and chlorovinyl, HCl, or chloroethyl sulfide radicals, which then decompose via a retro-ene reaction to produce vinyl chloride and thioacetaldehyde.[43] A literature search revealed studies on the decomposition of diethyl sulfide (DES), another common simulant for sulfur mustard, that under pyrolysis conditions, major products of DES thermal decomposition included ethylene, methane, ethane, and thioaldehydes.[24,44] While DES lacks both terminal chlorine atoms, CEES only lacks one terminal chlorine atom when compared to the structure of sulfur mustard. Based on these slight molecular differences, it follows that the resulting products of CEES decomposition would reasonably contain chloroethane and other hydrocarbons with chloride groups. Similar degradation mechanisms were found in the reaction of CEES and DES with oxidized porous carbon

https://dx.doi.org/10.1021/acsomega.0c01619
ACS Omega 2020, 5, 20051−20061

surfaces, supporting the hypothesis of cleaving of the C−S bond to both degrade the CWA and produce flammable secondary species.[24] Based on the known flammability of these products and the low bond energies of the C−S bonds in both the simulants and true agent, sulfur mustard, it is theorized that all of these compounds will readily decompose via thermal means.[43] The literature also shows that the primary products that are released from the thermal decomposition of HD are carbon monoxide, carbon dioxide, water, hydrogen gas, and hydrochloric acid.[38,43,44] Studies also concluded that while the boiling point of CEES is 156 °C, in experiments where the temperature reached above 350 °C, it was possible to degrade CEES, with complete degradation achieved at temperatures above 450 °C.[38,44] Fourier transform infrared (FTIR) spectra of the emitted vapors from experiments conducted with CEES at temperatures ranging from 20 to 80 °C confirmed that CEES was present in the emitted vapors and smoke (Figure S8). This study also found within 60 s of ignition that the concentration of CEES released into the atmosphere sharply decreases (Figure S9) as the liquid pool of simulant burns. This further supports that while there is initially a small release of CEES into the immediate environment, this is a short-term emission once the system reaches the appropriate temperature to cause decomposition by the previously mentioned pericyclic reaction. For the experiments where napalm-coated PyCBs were used as the ignition source, the temperature of the sample pan was measured with an infrared camera, revealing that the temperature varied between 350 and 400 °C. Based on the results of previous studies and the temperatures achieved with napalm-coated pyrolyzed cotton balls, it was inferred that the CEES used in these thermal decomposition experiments was also degraded into the less toxic products.

To test this scenario and demonstrate the utility of the use of PyCB, experiments were performed using CEES and varying the size of the burning pan. As a summary, Figure 5 shows the dependence of the maximum burning rate as a function of the pan diameter (n = 3).

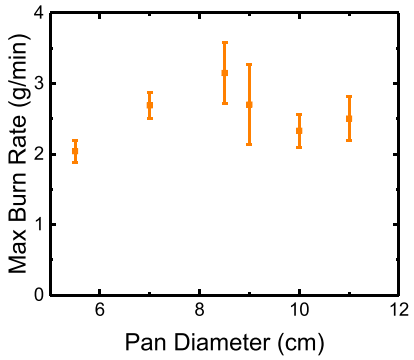

Figure 5. Comparison of the maximum burning rates achieved with PyCBs in CEES as a function of the diameter of the sample pan. The size of the pan does initially influence the maximum rate of burning achieved, but as the pans continue to increase in size, the rate of burning plateaus.

As observed in Figure 5, the maximum burning rate increases as a function of pan size from the 5.5 to 8.5 cm burning pans. Then, a decrease was observed, reaching a plateau when the 10.0 cm diameter pans were used. This suggests that there is a positive relationship between the surface area of the pan and the maximum rate of burning. However, if the volume of the bulk liquid agent is significantly greater than the volume of the substrate, which is introduced to initiate the burning, the lower temperature of the bulk simulant will depress the rate of burning. In other words, the energy released by burning one napalm-coated PyCB is not enough to cause continuously increasing rates of burning as the volume of agent in the pan increases. As a reference only, it is worth mentioning that a statistical analysis of the data shows that the maximum burning rate using the 8.5 cm pan is significantly different from the maximum burning rate using either the 5.5 cm pan (p = 0.004) or the 11 cm pan (p = 0.003). It is also important to state that during the burning of CEES, the maximum burning rate was achieved after 140 ± 20 s post ignition, with burning occurring across the entire surface area of the sample pan. Due to the limited volume of the syringe pump, this maximum burning rate was sustained only for an average of 90 ± 30 s. Across all burning pan sizes, over 50% of the total burned mass was consumed during this short period of maximum burning, although the maximum burning time accounted for only 20% of the total burning period. Based on previous research on the reactivity of simulants as compared to the reactivity of actual warfare agents, CWAs were found to be more reactive than their respective simulants,[45] and a similar trend is expected for the thermal decomposition of the agents. This suggests that H series agents will not only be able to sustain burning but also achieve the maximum burning rate within 2 min post ignition when a napalm-coated pyrolyzed cotton ball is used as the ignition source. It should be noted that once the entire surface area of the sample pan was ignited the agent would continue to burn until all of the sample was consumed. For the purposes of this study, data collected after the volume of sample in the syringe pump was depleted were excluded in the analysis of the burn rate.

Decomposition of TEP. To evaluate the efficacy of PyCBs to ignite other simulants, experiments were also performed using the simulant TEP while varying the size of the burning pan. As a summary, Figure 6 shows the dependence of the maximum burning rate as a function of the pan diameter. It can be observed that while the PyCBs were able to promote the thermal decomposition of TEP, which is generally considered a flame retardant,[41,46−48] the maximum burning rate only showed marginal increases (within the error of the method) as the pan size increased from 5.5 to 9.0 cm. This difference (with respect to the results obtained with CEES; Figure 5) was

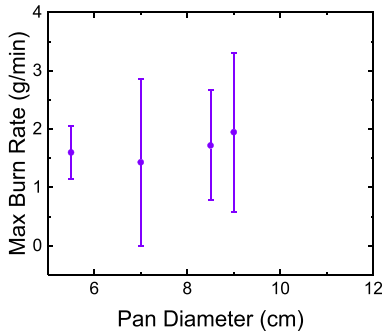

Figure 6. Comparison of maximum burning rates achieved with PyCBs in TEP as a function of the diameter of the sample pan. The size of the pan appears to have minimal impact on the rate of burning achieved when TEP is used.

https://dx.doi.org/10.1021/acsomega.0c01619
ACS Omega 2020, 5, 20051−20061

attributed to the lower reactivity of TEP. Additionally, TEP yielded a lower maximum burning rate (compared to CEES) across all burning pan diameters. To illustrate the challenges in igniting organophosphate-containing compounds, it is important to note that organophosphates are commonly used in flame retardants due to their stability, high flash points, and resistance to burning.[41,46−48] The presence of the phosphate functional group in both the simulant and the actual agents contributes to an increased flashpoint, making these nerve agents significantly more resistant toward combustion than the H series agents. Interestingly, the smallest pan (5.5 cm diameter) exhibited a much more consistent maximum burning rate across all repetitions (n = 3).

During the burning experiments, it was observed that a white layer of vapor was produced above the liquid agent, and in the smaller diameter pans, this vapor would ignite, resulting in sustained burning across the total surface area of the burning pan. The formation of this vapor, which was more pronounced in smaller pans, was attributed to a pericyclic reaction that results in the fragmentation of TEP, a retro-ene reaction, as proposed in Figure 7.[39,40,46,47,49] While the literature differs on

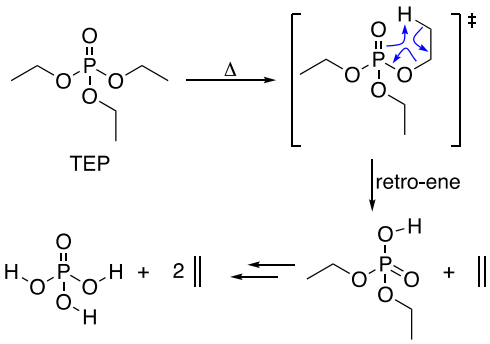

Figure 7. Proposed reaction mechanism for TEP generating flammable ethylene and the less toxic byproduct, phosphoric acid. This reaction requires the high temperatures from the burning of napalm to liberate the ethylene and to proliferate the reaction until all ethyl groups are removed, leaving only phosphoric acid. The blue arrows represent electron movement.

if the pericyclic reaction proceeds in a six-centered[47] or four-centered[46] pericyclic reaction, the expected byproducts are consistently ethylene, ethanol, and phosphoric acid. While the exact mechanism of decomposition has not been confirmed, the proposed mechanism suggests that the energy from the burning napalm causes the pericyclic reaction, resulting in the expulsion of highly flammable ethylene. The ethylene produced from this reaction is posited as the major fuel component in the decomposition of TEP and is continuously released by the proposed mechanism below, eventually producing the less toxic phosphoric acid. Previous studies on the kinetics of TEP decomposition in flow reactors identified the major products of pyrolysis over a temperature range of 427−627 °C as ethylene and ethanol.[46] These results suggest that at the temperature ranges observed with napalm-coated pyrolyzed cotton balls (250−450 °C) the liquid agent could decompose via the proposed pericyclic process and produce the flammable ethylene, thereby allowing the liquid simulant to serve as the fuel for the sustained thermal decomposition.

It is important to highlight that while the smallest pan size (5.5 cm diameter) used in this study was able to achieve complete burning across the entire pan surface area. Unlike CEES, however, the combustion reaction did not continue until all simulant in the sample pan was thermally decomposed in every trial. Several trials resulted in the agent extinguishing the incendiary agent on the pyrolyzed cotton balls prior to complete decomposition. It is posited that this extinguishing event is due to the energy from the napalm mixture burning being transferred to the liquid agent to warm it to its ignition point (above 110 °C) but not sufficient enough to cause sustained combustion of the simulant (above 230 °C). Further studies are needed to identify the effectiveness of different incendiary agents for maintaining the burning period for a greater amount of time. It is clear, however, that the pyrolyzed cotton ball substrate is critical to achieving any burning as all trials with unpyrolyzed cotton balls and napalm were unsuccessful, as the liquid agent rapidly quenched any flames and no discernible rate of burning was measured.

CONCLUSIONS

This paper describes the possibility to use carbon-based materials as substrates to thermally decompose different classes of chemical warfare agent simulants under ambient conditions. Not only are PyCBs able to serve as effective substrates for the delivery of relatively large volumes of an incendiary agent relative to the size and mass of the substrate itself, but they also increase the rate of decomposition when compared to the incendiary agent alone. Furthermore, PyCBs enable the decomposition of simulants with very limited byproducts. While further studies are required to confirm the exact composition of the gases and fumes produced by the thermal degradation of these compounds, the ability to rapidly decompose large volumes of these deadly substances is a significant improvement in the efforts to eliminate the stockpiles of these weapons at low cost. This study also presents a field-deployable method for decomposition of a broad range of chemical warfare agents with limited sample preparation or specialized training for the end user. In general, the structural changes induced by the pyrolysis of the cotton balls enhanced the ability of the napalm mixture to continuously combust when introduced into the pan containing the CWA simulants. This was due to its ability to increase the temperature of the surrounding agent to the point of ignition and allow the agent itself to fuel the combustion reaction, leading to complete decomposition of the simulants in pool fire experiments. By using the napalm-coated pyrolyzed cotton balls, it may be possible to eliminate the need for an external fuel source, such as an incinerator or butane torch, aiding in a more field-deployable thermal decomposition system. These results suggest that napalm-coated pyrolyzed cotton balls could serve as an effective method toward the thermal decomposition of bulk quantities of chemical warfare agents and their simulants; however, further studies are required to optimize the conditions for achieving thermal decomposition in large volumes of liquid agents.

EXPERIMENTAL SECTION

Selected Compounds. Due to the toxicity of chemical warfare agents and the extensive requirements necessary for their use in laboratory research, this study focused on the use of simulants in place of the agents themselves. These compounds have chemical structures and reactivity similar to the chemical warfare agents they model but with much lower toxicity.[25,50] It is also important to note that the use of

https://dx.doi.org/10.1021/acsomega.0c01619
ACS Omega 2020, 5, 20051−20061

simulants is common practice when studying chemical warfare agents, and multiple studies have shown that reactions with live agents generally proceed at a much higher rate than reactions with the simulants due to the presence of more reactive functional groups.[16,25,45,51,52] Therefore, we focused on the simulant 2-chloroethyl ethyl sulfide (CEES) for the blister agent sulfur mustard (HD) and triethyl phosphate (TEP) for the nerve agent sarin (GB). The simulants used in this study were purchased from either Sigma-Aldrich (St. Louis, MO) or TCI America (Portland, OR). All products were in 97.0% purity or greater and used as received. The napalm B, the incendiary agent in this study, was prepared by first mixing approximately gasoline (70%, 93 octane) and benzene (30%; Sigma-Aldrich, St. Louis, MO). Then, expanded polystyrene (from common packing peanuts) was added to the solution as a thickening agent at a ratio of 0.195 ± 0.002 g polystyrene (three packing peanuts) per 1 mL of gasoline/benzene mixture. This created a viscous and highly flammable solution that was able to provide the thermal energy required to start the decomposition of the various simulants. As the solvent is volatile, a fresh sample was prepared daily. It is important to note that other forms of polystyrene will work for the preparation of napalm B; however, our group found that packing peanuts dissolve faster in the solution than polystyrene pellets with no decrease in flammability.

Pyrolyzed Cotton Balls. Cotton balls (Up & Up brand, purchased from a local convenience store) were selected to serve as the substrate for the delivery of the incendiary agent due to their low weight, high cellulose content, and three-dimensional structure. To increase the hydrophobicity while maintaining the structure of the material, the cotton balls were pyrolyzed using a tube furnace (Thermolyne F21135, Barnstead International, Dubuque, IA) following a previously reported procedure.[34] The cotton balls were placed in the center of the furnace over a silicon wafer that acts as an inert holder. The ends of the quartz tube were then sealed and flushed for 5 min with forming gas (1 $L \cdot min^{-1}$ 95% Ar + 5% H_2, v/v) to remove the ambient air contained in the tube and generate a mildly reducing environment.[34] Next, the temperature was increased to 1000 °C at 30 $°C \cdot min^{-1}$. After 1 h at 1000 °C, the system was allowed to cool to room temperature and the resulting pyrolyzed cotton balls (PyCBs) were stored in Petri dishes until used. Pyrolysis of other brands of cotton balls has rendered materials with comparable properties.[53] It is also important to note that similar wicks can be fabricated without the need for a tube furnace (see the Supporting Information), further increasing the applicability of the material.

Control Experiments. To show that the increase in the rate of burning was a result of the pyrolyzed cotton ball wick, several control experiments were conducted. The first experiment used napalm added to the pool of simulant in a dropwise manner. In this experiment, a portion of the napalm mixture was scooped onto the end of a spatula, suspended over the pool of simulant, and ignited. Once the napalm sample was ignited, it dripped into the sample pan and the experiments continued, as described above in Figure 1. Controls were also conducted with napalm spread on a wire mesh and suspended above the surface of the agent in the sample pan. This experiment allowed for the determination of the impact that the incendiary agent alone had on inducing burning of the sample. To ensure accuracy, pyrolyzed cotton balls were coated with napalm and then weighed to determine the average amount of napalm that a pyrolyzed cotton ball could support. It was found that one pyrolyzed cotton ball supported 1.2 ± 0.1 g of napalm. The wire mesh was then coated with 1.2 ± 0.1 g of napalm, placed on the sample pan, and ignited once the syringe pump was turned on, and a consistent rate of overflow was established. This control was applied for both simulants examined in this study, CEES and TEP.

To compare the impact of pyrolyzing cotton balls, it was necessary to establish the rate of burning with unpyrolyzed cotton balls. In the first control with unpyrolyzed cotton balls, untreated cotton balls were ignited and placed in the sample pan as previously described. All other conditions were the same as previously described. In the second control, unpyrolyzed cotton balls were coated with napalm, ignited, and then placed in the sample pan as previously described. While the unpyrolyzed cotton balls were slightly burned due to the combustion of the napalm, the absence of a reducing atmosphere prevents the unpyrolyzed cotton balls from undergoing pyrolysis. All other conditions were the same as previously described. These controls were applied for both simulants examined in this study, CEES and TEP. Finally, to examine the impact of the structure of the pyrolyzed cotton balls on inducing burning, a pyrolyzed cotton ball was ground into a fine powder with a mortar and pestle. This powder was then added to 1.2 ± 0.1 g of napalm and thoroughly mixed. The suspension was then dried for 30 min and formed into a spherical pellet with a diameter of approximately 1 cm. Pellets were then ignited and placed in the sample pan as previously described. All other conditions were the same as previously described. These controls were applied for both simulants examined in this study, CEES and TEP. It is important to note that other sources of cellulose were examined in this study to determine if the starting material was critical to inducing burning. A Whatman type 3 chromatography paper was pyrolyzed in the same method as previously described for the cotton balls. However, the resulting pyrolyzed paper was not able to support the napalm mixture, and no measurable burning was detected in these experiments. Following these experiments, it was concluded that the three-dimensional structure of the cotton balls was critical to its role as both a wick and a substrate for the delivery of the napalm mixture.

Pyrolyzed Cotton Ball Characterization. Pyrolyzed cotton ball samples were characterized for their surface area, average pore diameter, and physical structure to determine the effect that pyrolyzing the cotton balls had on the ability of the substrate to wick the simulants. Surface area and pore diameter measurements were conducted via the widely accepted method of nitrogen adsorption isotherms and the application of the Brunauer–Emmett–Teller (BET) and Barrett–Joyner–Halenda (BJH) methods.[35,36] The nitrogen adsorption isotherm and pore size analysis were conducted using an Autosorb IQ (Quantachrome Instruments, Ashland, VA). Samples were outgassed under vacuum for 5 h at 300 °C to remove any impurities from sample pores. Scanning electron microscope (S3400 and SU6600, Hitachi High Technologies, Pleasanton, CA) imaging was conducted to compare changes in the physical structure of the cotton balls as a result of the pyrolyzation process.

Optical imaging was conducted at the Clemson Light Imaging Facility (CLIF) by a trained technician with an Olympus OLS5000 LEXT optical profiler (Olympus Corporation, Tokyo, Japan). Through this analysis, it was possible to estimate the roughness of the pyrolyzed cotton balls and the

https://dx.doi.org/10.1021/acsomega.0c01619
ACS Omega 2020, 5, 20051−20061

width of the fibers. In this study, a pyrolyzed cotton ball was segmented into six pieces to confirm the consistency of the structural features throughout the pyrolyzed cotton ball. While it was not possible to construct a three-dimensional rendering of the pyrolyzed cotton ball, through this imaging technique, it was possible to view the layering and interconnections between the individual strands of the pyrolyzed cellulose fibers.

■ ASSOCIATED CONTENT

Supporting Information

The Supporting Information is available free of charge at https://pubs.acs.org/doi/10.1021/acsomega.0c01619.

Alternative routes for the fabrication of carbon wicks; alternative views of the experimental setup for the burning of chemical warfare agent simulants while measuring overflow, where the $CaCO_3$ shield is more visible; scanning electron microscope image of non-pyrolyzed cotton ball fibers (left) and pyrolyzed cotton ball fibers (right); optical noncontact roughness measurements of the interior structure of the pyrolyzed cotton ball; BET isotherm for pyrolyzed cotton balls and pore size distribution; image of the pyrolyzed cotton ball with a drop of water; FTIR spectrum of CEES vapor from experiments conducted below 80 °C; and concentration of CEES in gas phase over time (PDF)

■ AUTHOR INFORMATION

Corresponding Authors

Matthew S. Blais − *Southwest Research Institute, San Antonio, Texas 78238, United States*; Email: matthew.blais@swri.org

Carlos D. Garcia − *Department of Chemistry, Clemson University, Clemson, South Carolina 29634, United States*; orcid.org/0000-0002-7583-5585; Email: cdgarci@clemson.edu

Authors

Bryan A. Lagasse − *Department of Chemistry, Clemson University, Clemson, South Carolina 29634, United States; Department of Chemistry and Life Science, United States Military Academy, West Point, New York 10996, United States*

Laura McCann − *Department of Chemistry, Clemson University, Clemson, South Carolina 29634, United States*

Timothy Kidwell − *Southwest Research Institute, San Antonio, Texas 78238, United States*

Complete contact information is available at: https://pubs.acs.org/10.1021/acsomega.0c01619

Notes

The authors declare no competing financial interest.

■ ACKNOWLEDGMENTS

Funding for this project was provided in part by Clemson University and by the Defense Threat Reduction Agency contract # HDTRA1-16-1-0030, via Southwest Research Institute.

■ REFERENCES

(1) Borak, J.; Sidell, F. R. Agents of Chemical Warfare: Sulfur Mustard. *Ann. Emerg. Med.* **1992**, *21*, 303−308.

(2) Blewett, W. Tactical Weapons: Is Mustard Still King? *NBC Def. Technol. Int.* **1986**, *1*, 64−66.

(3) Giannakoudakis, D. A.; Bandosz, T. J. *Detoxification of Chemical Warfare Agents*; Springer: Cham, 2018.

(4) Gilman, A.; Phillips, F. S. The Biological Actions and Therapeutic Applications of the B-Chloroethyl Amines and Sulfides. *Science* **1946**, *103*, 409−415.

(5) Dunn, P. The Chemical War: Iran Revisited 1986. *NBC Def. Technol. Int.* **1986**, *1*, 32−39.

(6) McNaugher, T. L. Ballistic Missles and Chemical Weapons: The Legacy of the Iran-Iraq War. *Int. Secur.* **1990**, *15*, 5−34.

(7) *Chemical Agent Data Sheets*; U.S. Department of the Army, 1974; Vol. *1*.

(8) Munro, N. B.; Ambrose, K. R.; Watson, A. P. Toxicity of the Organophosphate Chemical Warfare Agents GA, GB, and VX: Implications for Public Protection. *Environ. Health Perspect.* **1994**, *102*, 18−38.

(9) Kloske, M.; Witkiewicz, Z. Novichoks − The A Group of Organophosphorus Chemical Warfare Agents. *Chemosphere* **2019**, *221*, 672−682.

(10) Grob, D.; Harver, A. M. The Effects and Treatment of Nerve Gas Poisoning. *Am. J. Med.* **1953**, *14*, 52−63.

(11) Howkrs, M. B., Jr.; Goodman, E. M. S.; Sim, V. M. Some Behavioral Changes in Man Following Anticholinesterase Administration. *J. Nerv. Ment. Dis.* **1964**, *138*, 383−389.

(12) Munro, N. B.; Watson, A. P.; Ambrose, K. R.; Griffin, G. D. Treating Exposure to Chemical Warfare Agents: Implications for Health Care Providers and Community Emergency Planning. *Environ. Health Perspect.* **1990**, *89*, 205−215.

(13) Love, A. H.; Vance, A. L.; Reynolds, J. G.; Davisson, M. L. Investigating the Affinities and Persistence of VX Nerve Agent in Environmental Matrices. *Chemosphere* **2004**, *57*, 1257−1264.

(14) Schneider, T.; Lütkefend, T. *Nowhere to Hide: The Logic of Chemical Weapons Use in Syria*; Global Public Policy Institute: 2019.

(15) Yang, Y. C.; Baker, J. A.; Ward, R. Decontamination of Chemical Warfare Agents. *Chem. Rev.* **1992**, *92*, 1729−1743.

(16) Yang, Y. C. Chemical Detoxification of Nerve Agent VX. *Acc. Chem. Res.* **1999**, *32*, 109−115.

(17) Jõul, P.; Vaher, M.; Kuhtinskaja, M. Evaluation of Carbon Aerogel-Based Solid-Phase Extraction Sorbent for the Analysis of Sulfur Mustard Degradation Products in Environmental Water Samples. *Chemosphere* **2018**, *198*, 460−468.

(18) Petrea, N.; Petre, R.; Epure, G.; Şomoghi, V.; TĂnase, L. C.; Teodorescu, C. M.; Neaţu, Ş. The Combined Action of Methanolysis and Heterogeneous Photocatalysis in the Decomposition of Chemical Warfare Agents. *Chem. Commun.* **2016**, *52*, 12956−12959.

(19) Kim, M. K.; Kim, S. H.; Park, M.; Ryu, S. G.; Jung, H. Degradation of Chemical Warfare Agents over Cotton Fabric Functionalized with UiO-66-NH 2. *RSC Adv.* **2018**, *8*, 41633−41638.

(20) U.S. Congress Office of Technology Assessment. *Disposal of Chemical Weapons: Alternative Technologies-Background Paper*, OTA-BP-O-95; U.S. Government Printing Office: Washington, DC, 1992.

(21) Flamm, K. J.; Kwan, Q.; McNulty, W. B. *Chemical Agent and Munition Disposal: Summary of the U.S. Army's Experience*; Office of the Program Manager for Chemical Demilitarization: Aberdeen ProvingGround, MD, 1987.

(22) Bobbitt, N. S.; Mendonca, M. L.; Howarth, A. J.; Islamoglu, T.; Hupp, J. T.; Farha, O. K.; Snurr, R. Q. Metal-Organic Frameworks for the Removal of Toxic Industrial Chemicals and Chemical Warfare Agents. *Chem. Soc. Rev.* **2017**, *46*, 3357−3385.

(23) Zhao, J.; Lee, D. T.; Yaga, R. W.; Hall, M. G.; Barton, H. F.; Woodward, I. R.; Oldham, C. J.; Walls, H. J.; Peterson, G. W.; Parsons, G. N. Ultra-Fast Degradation of Chemical Warfare Agents Using MOF−Nanofiber Kebabs. *Angew. Chem., Int. Ed.* **2016**, *55*, 13224−13228.

(24) Florent, M.; Giannakoudakis, D. A.; Bandosz, T. J. Mustard Gas Surrogate Interactions with Modified Porous Carbon Fabrics: Effect of Oxidative Treatment. *Langmuir* **2017**, *33*, 11475−11483.

(25) Picard, B.; Chataigner, I.; Maddaluno, J.; Legros, J. Introduction to Chemical Warfare Agents, Relevant Simulants and

Modern Neutralisation Methods. *Org. Biomol. Chem.* **2019**, *17*, 6528−6537.
(26) Singh, B.; Prasad, G. K.; Pandey, K. S.; Danikhel, R. K.; Vijayaraghavan, R. Decontamination of Chemical Warfare Agents. *Def. Sci. J.* **2010**, *60*, 428−441.
(27) Zhang, W.; Sun, H.; Chen, W.; Zhang, Y.; Wang, F.; Tang, S.; Zhang, J.; Wang, H.; Wang, R. Mechanistic and Kinetic Study on the Reaction of Ozone and Trans-2-Chlorovinyldichloroarsine. *Chemosphere* **2016**, *150*, 329−340.
(28) Sharma, V. K.; Luther, G. W.; Millero, F. J. Mechanisms of Oxidation of Organosulfur Compounds by Ferrate(VI). *Chemosphere* **2011**, *82*, 1083−1089.
(29) Li, Y.; Gao, Q.; Zhou, Y.; Zhang, L.; Zhong, Y.; Ying, Y.; Zhang, M.; Liu, Y.; Wang, Y. Significant Enhancement in Hydrolytic Degradation of Sulfur Mustard Promoted by Silver Nanoparticles in the Ag NPs@HKUST-1 Composites. *J. Hazard. Mater.* **2018**, *358*, 113−121.
(30) Verma, A. K.; Srivastava, A. K.; Singh, B.; Shah, D.; Shrivastava, S.; Shinde, C. K. P. Alumina-Supported Oxime for the Degradation of Sarin and Diethylchlorophosphate. *Chemosphere* **2013**, *90*, 2254−2260.
(31) Sides, G. D.; Manier, M. L. Pyrolysis of Bis(2-chloroethyl) Sulfide (HD), 1985. Report prepared by Southern Research Institute for GA Technologies, Inc. under contract DAAK11-84-C-0028.
(32) Sides, G.; Manier, M. L.; Spafford, R. B. The Pyrolysis of VX, GB, and HD Trapped in Stainless Steel Reaction Vessels, 1986. Report prepared by Southern Research Institute for GA Technologies, Inc. under contract DAAK11-84-C-0028.
(33) Zavitsanos, P.; Rozanski, A.; Files, C.; Stotz, N. Destruction of CWA by Wicking Compound and High Temperature Incendiary. US9,610,468B2, 2017.
(34) Benavidez, T. E.; Martinez-Duarte, R.; Garcia, C. D. Analytical Methodologies Using Carbon Substrates Developed by Pyrolysis. *Anal. Methods* **2016**, *8*, 4163−4176.
(35) Long, D.; Zhang, R.; Qiao, W.; Zhang, L.; Liang, X.; Ling, L. Biomolecular Adsorption Behavior on Spherical Carbon Aerogels with Various Mesopore Sizes. *J. Colloid Interface Sci.* **2009**, *331*, 40−46.
(36) Özdemir, M.; Bolgaz, T.; Saka, C.; Şahin, Ö. Preparation and Characterization of Activated Carbon from Cotton Stalks in a Two-Stage Process. *J. Anal. Appl. Pyrolysis* **2011**, *92*, 171−175.
(37) Giuliani, J. G.; Benavidez, T. E.; Duran, G. M.; Vinogradova, E.; Rios, A.; Garcia, C. D. Development and Characterization of Carbon Based Electrodes from Pyrolyzed Paper for Biosensing Applications. *J. Electroanal. Chem.* **2016**, *765*, 8−15.
(38) Wagner, G. W.; Maciver, B. K.; Rohrbaugh, D. K.; Yang, Y. C. Thermal Degradation of Bis (2-Chloroethyl) Sulfide (Mustard Gas). *Phosphorus, Sulfur Silicon Relat. Elem.* **1999**, *152*, 65−76.
(39) Paderes, G. D.; Jorgensen, W. L. Computer-Assisted Mechanistic Evaluation of Organic Reactions. 20. Ene and Retro-Ene Chemistry. *J. Org. Chem.* **1992**, *57*, 1904−1916.
(40) Bruffaerts, J.; Vasseur, A.; Marek, I. Alkene-Zipper Catalyzed Selective and Remote Retro-Ene Reaction of Alkenyl Cyclopropylcarbinol. *Adv. Synth. Catal.* **2018**, *360*, 1389−1396.
(41) Deng, J.; Zhang, P.; Jin, T.; Zhou, H.; Cheng, J. Graphene Oxide/β-Cyclodextrin Composite as Fiber Coating for High Efficiency Headspace Solid Phase Microextraction of Organophosphate Ester Flame Retardants in Environmental Water. *RSC Adv.* **2017**, *7*, 54475−54484.
(42) Yuan, X.; Lacorte, S.; Cristale, J.; Dantas, R. F.; Sans, C.; Esplugas, S.; Qiang, Z. Removal of Organophosphate Esters from Municipal Secondary Effluent by Ozone and UV/H2O2 Treatments. *Sep. Purif. Technol.* **2015**, *156*, 1028−1034.
(43) Sirjean, B.; Lizardo-Huerta, J. C.; Verdier, L.; Fournet, R.; Glaude, P. A. Kinetic Modeling of the Thermal Destruction of Mustard Gas. *Proc. Combust. Inst.* **2017**, *36*, 499−506.
(44) Zheng, X.; Fisher, E. M.; Gouldin, F. C.; Zhu, L.; Bozzelli, J. W. Experimental and Computational Study of Diethyl Sulfide Pyrolysis and Mechanism. *Proc. Combust. Inst.* **2009**, *32*, 469−476.
(45) Kumar, V.; Raviraju, G.; Rana, H.; Rao, V. K.; Gupta, A. K. Highly Selective and Sensitive Chromogenic Detection of Nerve Agents (Sarin, Tabun and VX): A Multianalyte Detection Approach. *Chem. Commun.* **2017**, *53*, 12954−12957.
(46) Glaude, P. A.; Curran, H. J.; Pitz, W. J.; Westbrook, C. K. Kinetic Study of the Combustion of Organophosphorus Compounds. *Proc. Combust. Inst.* **2000**, *28*, 1749−1756.
(47) Zegers, E. J. P.; Fisher, E. M. Pyrolysis of Triethyl Phosphate. *Combust. Sci. Technol.* **1998**, *138*, 85−103.
(48) Neupane, S.; Rahman, R. K.; Masunov, A. E.; Vasu, S. S. Theoretical Calculation of Reaction Rates and Combustion Kinetic Modeling Study of Triethyl Phosphate (TEP). *J. Phys. Chem. A* **2019**, *123*, 4764−4775.
(49) Neupane, S.; Barnes, F.; Barak, S.; Ninnemann, E.; Loparo, Z.; Masunov, A. E.; Vasu, S. S. Shock Tube/Laser Absorption and Kinetic Modeling Study of Triethyl Phosphate Combustion. *J. Phys. Chem. A* **2018**, *122*, 3829−3836.
(50) Kim, K.; Tsay, O. G.; Atwood, D. A.; Churchill, D. G. Destruction and Detection of Chemical Warfare Agents. *Chem. Rev.* **2011**, *111*, 5345−5403.
(51) Bartelt-Hunt, S. L.; Knappe, D. R. U.; Barlaz, M. A. A Review of Chemical Warfare Agent Simulants for the Study of Environmental Behavior. *Crit. Rev. Environ. Sci. Technol.* **2008**, *38*, 112−136.
(52) Wallace, K. J.; Morey, J.; Lynch, V. M.; Anslyn, E. V. Colorimetric Detection of Chemical Warfare Simulants. *New J. Chem.* **2005**, *29*, 1469−1474.
(53) Reed, P. A.; Cardoso, R. M.; Muñoz, R. A. A.; Garcia, C. D. Pyrolyzed Cotton Balls for Protein Removal: Analysis of Pharmaceuticals in Serum by Capillary Electrophoresis. *Anal. Chim. Acta* **2020**, *1110*, 90−97.

https://dx.doi.org/10.1021/acsomega.0c01619
ACS Omega 2020, 5, 20051−20061